Numerical Simulation of Gravel Packing

P.H. Winterfeld, SPE, and **D.E. Schroeder Jr.,** SPE, Marathon Oil Co.

Summary. To obtain maximum productivity from unconsolidated formations where sand control is required, it is important to understand the mechanics of gravel packing. This paper describes a finite-element, numerical simulator that can predict gravel placement in the perforations and annulus of a wellbore. The equations for the simulator include mass and momentum conservation. Wellbore geometry, physical properties, and fluid and gravel-pack properties are simulator input. Experiments in a 100-ft full-scale wellbore model for three gravel-packing configurations have been successfully simulated. These configurations are a circulating pack with a washpipe, a squeeze pack, and a circulating/squeeze pack with a washpipe and a lower telltale screen. The low cost, speed, and extrapolation capabilities of the numerical simulator will greatly enhance our ability to predict gravel placement in a wellbore.

Introduction

Many gravel-packing procedures produce less-than-desirable results because of incomplete placement of gravel around the screen, particularly when the wellbore is deviated. With the onset of production in deeper water, highly deviated completions in unconsolidated formations are becoming commonplace. To obtain high productivity and to reduce water and gas coning, many wells are being drilled horizontally. Although the need for good sand control in these types of wells is critical, the chances of packing gravel over the entire screen in such a well are not very good.[1,2]

Numerous investigators have explored various aspects of obtaining a good gravel pack. Many have constructed experimental models for studying gravel packing,[3-11] but only a few have attempted to develop a mathematical model for predicting gravel placement.

Gruesbeck and Collins[3] developed generalized transport-efficiency correlations to predict particle transport into perforations for full-scale systems. These correlations indicate that relatively good gravel transport to the perforations can be obtained with moderate fluid viscosities and flow rates.

Gruesbeck *et al.*[4] developed two empirical relationships for equilibrium velocity of solids and pressure gradient in flowing slurry. These relationships were combined with steady-state mass and momentum balances to yield a mathematical model of gravel placement in a wellbore. Predictions were verified with a 20-ft wellbore model with a 5.5-in. ID containing a 2.875-in.-OD wire-wrapped screen. Later, Hodge[6] developed a computer program to predict equilibrium bank height based on slurry pressure gradient and equilibrium velocity relationships.

Peden *et al.*[7,12] used dimensional analysis to derive equations for annular-pack and perforation-pack efficiency. Coefficients for these equations were evaluated with experimental data from an 8-ft wellbore model with a 6-in. ID.[13] They found that an equilibrium bank would not be generated for carrier fluids with viscosity greater than 10 cp. Daneshy[13] found that high-viscosity (100-cp) fluids can transport sand (40/60 mesh) with almost no settling.

Wahlmeier and Andrews[14] developed a pseudo-3D mathematical model to aid in the design and evaluation of gravel packs. The mathematical model was validated with experimental results from an 18-ft, 6.2-in.-diameter wellbore model.

Wellbore Model

In 1985, a full-scale wellbore model was built at Marathon's E&P Technology facility in Littleton, CO.[15] The model consists of twenty 5-ft acrylic sections (casing) that can be assembled into wellbores up to 100 ft long. The ID of an acrylic section is 6.2 in. Eight of the acrylic sections are fitted with perforations. The perforations (**Fig. 1**) are 0.87 in. in diameter and 15 in. long. The porous polyethylene filter element represents the formation. Leakoff fluid flows through the filter element and is collected in a manifold. There is one manifold for each acrylic section. Perforations are arranged on a spiral with 90° phasing and a density of 8 perforations/ft.

The numerical simulator was used to match results from three gravel-packing configurations: a squeeze pack, a circulating pack, and a circulating/squeeze pack. In the squeeze-pack configuration (**Fig. 2**), the model has 5 ft of blank casing, followed by 35 ft of perforated casing and 50 ft of blank casing. An eight-gauge (0.008-in.) wire-wrapped main screen, which overlaps the perforations 5 ft above and below, is installed in the model. The main screen is wrapped on a 3.5-in. base pipe and has a 4.0-in. OD. The volume inside the main screen communicates only with the annulus. The total length of the model in this configuration is 90 ft.

The circulating configuration is similar to the squeeze configuration, except that a 2.38-in.-OD washpipe is installed inside the main screen. The bottom of the washpipe is located a few inches above the bottom of the main screen. The volume between the main screen and washpipe communicates with the annulus through the screen and the surroundings through the washpipe.

In the circulating/squeeze configuration (**Fig. 3**), an additional 5 ft of blank casing and telltale screen is added to the bottom of the model. A 2.38-in.-OD washpipe is installed inside the main screen. The volume between the main screen and washpipe communicates only with the annulus; the volume inside the telltale screen communicates with the annulus through the screen and with the surroundings by means of the washpipe. The total length of the model in this configuration is 95 ft.

A typical pumping sequence used in the experiments included 2 bbl of water, followed by 3 bbl of prepad, the appropriate quantity of slurry, and finally the push pad. The pump rate was 2 bbl/min. In the circulating/squeeze experiment, sandout across the telltale screen occurred first. Then, after a small amount of axial packing, little additional fluid flowed through the telltale screen. All injected fluid then was squeezed into the perforations. Finally, as the slurry flow path became restricted, a sandout was reached at the top of the main screen. Hydroxyethylcellulose (HEC) polymer was used in these experiments at a concentration of either 0.06 or 0.08 lbm/gal. Pressure and flow data were collected every 2 seconds during an experiment. Three mobile videocameras were used to record the progress of a gravel-pack experiment. The amount of gravel in the annulus and perforations was measured after an experiment.

Simulator Formulation

Fluid flow in the system and gravel packing on screen and in perforations are simulated. Slurry is a suspension of incompressible gravel particles in compressible liquid (carrier fluid). Liquid is typically a dilute solution of polymer, such as HEC, in water. At higher shear rates, liquid viscosity obeys the Ostwald-de Waele power-law model; at lower shear rates, liquid viscosity is approximately constant and is a maximum:

$$\mu = K|\dot{\gamma}|^{n-1} \le \mu_{max}. \quad \ldots\ldots\ldots\ldots\ldots\ldots\ldots\ldots\ldots\ldots (1)$$

Typically, this change from a constant-viscosity to a power-law model occurs at a shear rate of about 1 second^{-1}.

Slurry Flow in Annulus. A mass balance around a cross-sectional slice of slurry in the annulus yields

$$\frac{\partial}{\partial z}(\rho y)_j q_z + \dot{m}_j + \pi \frac{\partial}{\partial t}[(\rho y)_j (r_o^2 - r_i^2)] = 0, \quad j = L,g, \quad \ldots\ldots (2)$$

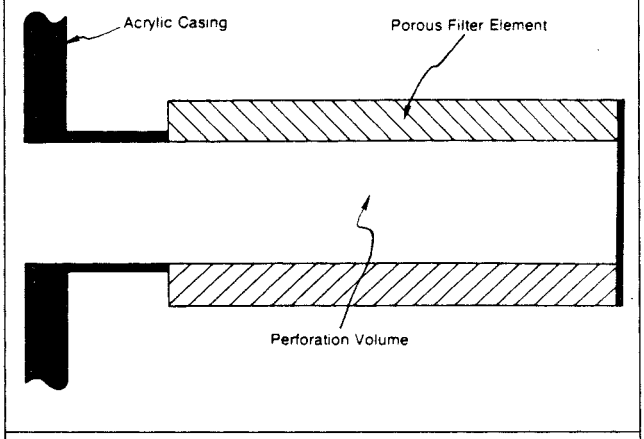

Fig. 1—Diagram of a perforation.

where r_o and r_i = outer and inner radii of the gravel pack, respectively, and $\dot{m}$ = rate of mass exchange per unit length to the surroundings. For example, mass loss to the surroundings occurs during gravel packing. Gravel-pack growth from screen causes r_i to increase; that from perforations causes r_o to decrease.

Conservation of momentum is for steady-state flow of a power-law fluid in an annulus:

$$q_z+\pi r_o^3\Omega\left(\frac{1}{n},\frac{r_i}{r_o}\right)\left\{\frac{r_o}{2K}\left[\frac{\partial p}{\partial z}-(y_L\rho_L+y_g\rho_g)\frac{g}{g_c}\cos\theta\right]\right\}^{1/n}=0, \quad \ldots\ldots\ldots\ldots (3)$$

where Ω is a tabulated function.[16]

Gravel-Pack Growth From Screen. Screen and gravel packs are permeable only to liquid. Hence, when slurry impinges on the leading surface of a gravel pack, the liquid portion passes through the leading surface into the porous gravel pack and the gravel portion is deposited at the leading surface, causing the gravel pack to grow. Mass balances around the leading surface of the growing gravel pack are

$$q_i y_g+\pi(y_g-y_g^p)(\partial r_i^2/\partial t)=0 \quad \ldots\ldots\ldots\ldots (4)$$

and $$q_i=q_i^p=0, \quad \ldots\ldots\ldots\ldots (5)$$

where q_i = volumetric flow rate per unit length of slurry impinging on the leading surface of the gravel pack, q_i^p = volumetric flow rate per unit length in the gravel pack of liquid at the gravel-pack leading surface, and y^p = volume fraction in the gravel pack.

Liquid flows radially inward through the gravel pack and out the annulus through the screen. Flow is presumed incompressible and steady-state. Expressions for q^p are derived by treating the screen and gravel pack as two flow resistances in series. For a power-law fluid flowing through N resistances in series,

$$(q^p)^n=\frac{p_N-p_0}{\sum_{i=1}^{N}\frac{1}{A_i}}, \quad \ldots\ldots\ldots\ldots (6)$$

where flow through the ith resistor is given by

$$(q^p)^n=A_i(p_i-p_{i-1}). \quad \ldots\ldots\ldots\ldots (7)$$

For gravel packs, the coefficient A_i is calculated from the analog of Darcy's law for radial flow of a power-law fluid through a porous medium[17]:

$$(v_r)^n=-7.322\times10^{-8}\frac{k_p}{\mu_e}\frac{\partial p}{\partial r}, \quad \ldots\ldots\ldots\ldots (8)$$

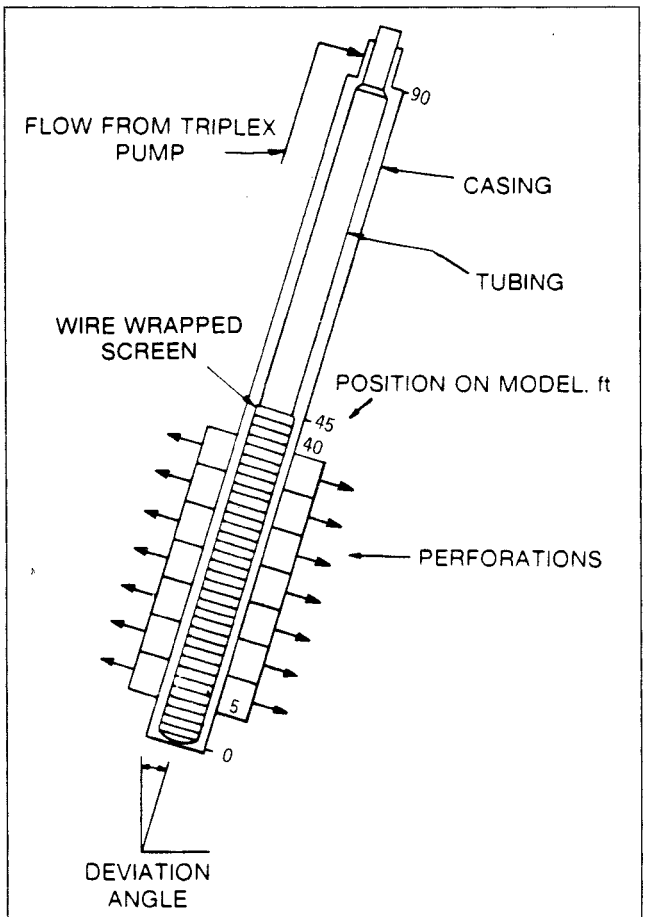

Fig. 2—Diagram of wellbore model in squeeze configuration.

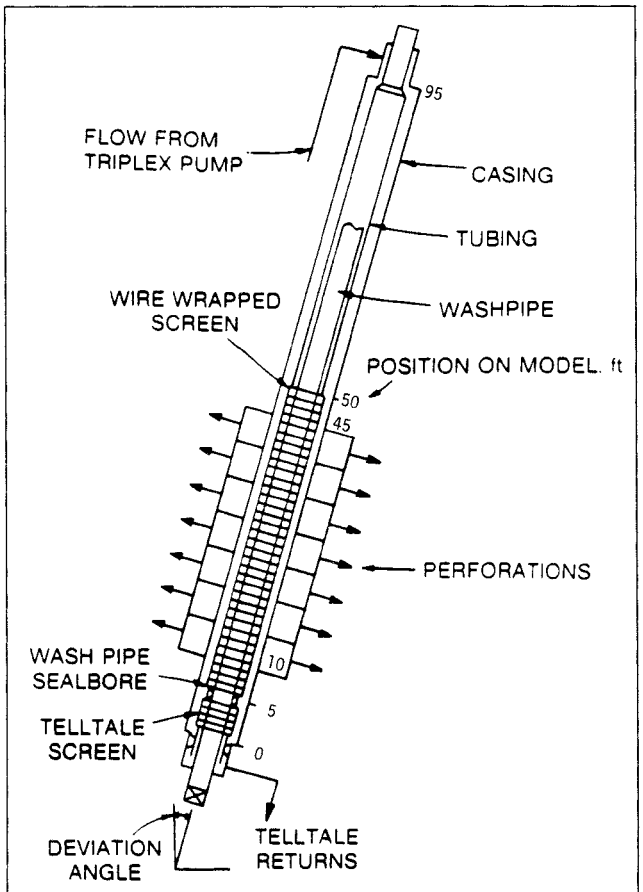

Fig. 3—Diagram of wellbore model in circulating/squeeze configuration.

where the effective viscosity, μ_e, is given by[18]

$$\mu_e=\frac{K}{12}\left(9+\frac{3}{n}\right)^n(1.593\times10^{-12}k_p y_L^p)^{(1-n)/2}. \quad \ldots\ldots\ldots(9)$$

The coefficient A_i of screen is constant.

Gravel-Pack Growth in Perforations. Perforations are approximated as an annulus of perforation volume that surrounds the perforated acrylic sections. If the outer radius of the perforation volume is imagined to be bounded by screen, gravel packing in perforations is similar to gravel-pack growth from screen. Corresponding mass balances are

$$q_o y_g-\pi(y_g-y_g^p)(\partial r_o^2/\partial t)=0 \quad \ldots\ldots\ldots(10)$$

and $q_o-q_o^p=0. \quad \ldots\ldots\ldots(11)$

Expressions for q_o^p are derived from perforation geometry. A perforation wall consists of two sections, an impermeable one for a short distance starting from the base on the acrylic section, which represents the casing and cement sheath of the wellbore, followed by the inside of an annular, porous filter element. Gravel packing in a perforation is assumed to proceed sequentially in this manner: first, radially inward from the surface of the filter element; next, axially from the start of the filter element to the base of the acrylic section; and then radially inward from the inner surface of the perforated acrylic sections. As in the case of gravel-pack growth from screen, liquid flows through several resistances in series, namely, through gravel packed on the surface of the perforated acrylic sections, the portion of the gravel-packed perforation from the base of the acrylic section to the start of the filter element, the portion of the gravel-packed perforation contacting the filter element, and then the filter element itself. Eqs. 8 and 9 and the axial analog of Eq. 8 are used to calculate coefficients A_i for each of these resistances. Results for one perforation then are multiplied by the number of perforations per unit axial length.

Evaluation of Mass Exchange Terms. The term $\dot{m}$ in Eq. 2 accounts for mass exchange between the slurry and the surroundings. The term has two contributors, one associated with screen on the inner radius of the annulus, $\dot{m}_i$, and the other with perforations, $\dot{m}_o$, where

$$\dot{m}_j=\dot{m}_{i,j}+\dot{m}_{o,j},\ j=L,g. \quad \ldots\ldots\ldots(12)$$

Mass exchange has two components, one from slurry impinging on the leading surface of the gravel pack and the other from the volume of slurry lost because the gravel pack is growing:

$$\dot{m}_{i,j}=(\rho y)_j[q_i^p+\pi(\partial r_i^2/\partial t)] \quad \ldots\ldots\ldots(13)$$

and $\dot{m}_{o,j}=(\rho y)_j[q_o^p-\pi(\partial r_o^2/\partial t)]. \quad \ldots\ldots\ldots(14)$

TABLE 1—PARAMETERS USED IN GRAVEL-PACKING SIMULATIONS

Polymer and Gravel Properties			
HEC concentration (lbm/gal)	K	n	μ_{max}
0.06	5,889	0.353	5,889
0.08	14,125	0.289	14,125
Gravel-grain density, lbm/ft³			165.4
Liquid density, lbm/ft³			62.4 + 0.0002p
System Properties			
Screen resistance, (ft/sec)^n/psi			1.0
Perforation radius, ft			0.0365
Total perforation length, ft			1.25
Perforation density, perforations/ft			8
Filter-element permeability, md			15,000
Filter-element porosity			0.5
Filter-element thickness, ft			0.0469
Filter-element length, ft			0.9479
Slurry flow rate, bbl/min			2
Initial pressure, psi			50

If the pressure drop between the annulus and the surroundings is negative, liquid flows into the annulus and there is no gravel-pack erosion.

Axial Gravel-Pack Growth. Gravel packs from perforations and screen, restricting slurry flow in the annulus. Eventually, the annulus is blocked by gravel pack. Afterward, gravel packs in an axial fashion in the annulus. Slurry impinges on the leading surface of the blocking gravel pack. The liquid portion passes through the leading surface into the porous gravel pack, and the gravel portion is deposited at the leading surface, causing the gravel pack to grow. Mass balances around the leading surface of the growing gravel pack are

$$y_g q_z-A_{cxn}(y_g-y_g^p)(\partial z_f/\partial t)=0 \quad \ldots\ldots\ldots(15)$$

and $q_z=q_z^p$ at $z=z_f, \quad \ldots\ldots\ldots(16)$

where z_f = location of the gravel-pack leading surface, q_z^p = volumetric flow rate of liquid in the gravel pack, and A_{cxn} = cross-sectional area of the annulus.

Liquid flows axially through the completely packed portion of the annulus. Conservation of mass is

$$(\partial/\partial z)(\rho_{Lq_z}^p)+\dot{m}_p+A_{cxn}y_L^p(\partial\rho_L/\partial t)=0. \quad \ldots\ldots\ldots(17)$$

Conservation of momentum is

$$q_z^p+A_{cxn}\left[\frac{k_p}{\mu_e}\left(\frac{\partial p}{\partial z}-\rho_L\frac{g}{g_c}\cos\theta\right)\right]^{1/n}=0. \quad \ldots\ldots\ldots(18)$$

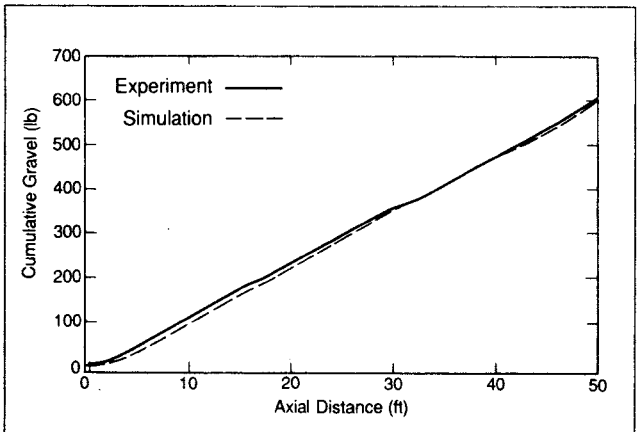

Fig. 4—Match of cumulative gravel distribution for circulating configuration.

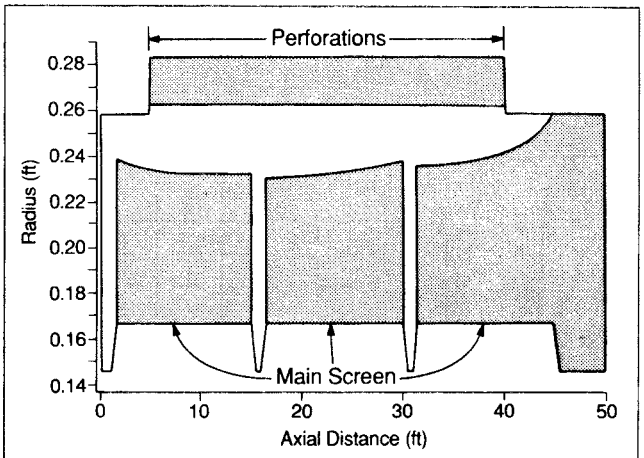

Fig. 5—Cross section of annulus for circulating configuration. Shaded area is gravel pack.

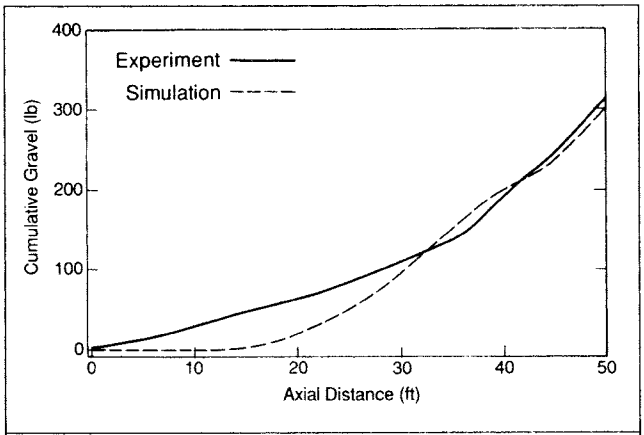

Fig. 6—Match of cumulative gravel distribution for squeeze configuration.

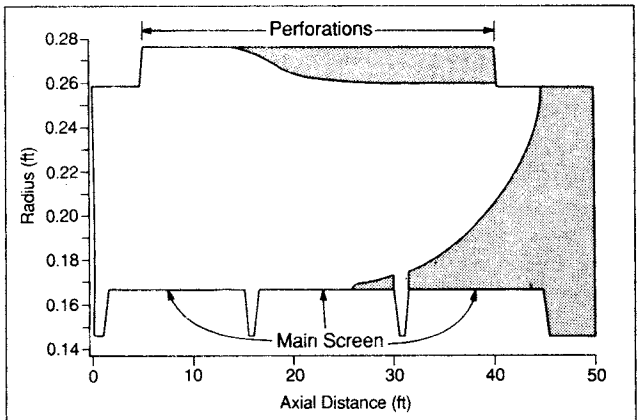

Fig. 7—Cross section of annulus for squeeze configuration. Shaded area is gravel pack.

The rate of liquid exchange per unit length to the surroundings, $\dot{m}_p$, is

$$\dot{m}_p = \rho_L \left[q_i^p \Big|_{r_i=(r_i^0+r_o^0)/2} + q_o^p \Big|_{r_o=(r_i^0+r_o^0)/2} \right]. \quad \ldots\ldots\ldots (19)$$

Liquid Flow in the System. Liquid leaving the annulus through the screen enters either the washpipe or the volume between the main screen and the washpipe. Both volumes have an annular cross section and contain no gravel. Mass and momentum conservation are Eqs. 2 and 3, respectively, with liquid volume fraction unity. The mass exchange term, $\dot{m}_{i,L}$, is

$$\dot{m}_{i,L} = -(\rho y)_L \left(q_i^p + \pi \frac{\partial r_i^2}{\partial t} \right) + \pi \rho_L y_L^p \frac{\partial r_i^2}{\partial t}, \quad \ldots\ldots\ldots (20)$$

the negative of the term for liquid lost from the annulus, Eq. 13, plus an additional term that accounts for liquid trapped in the growing gravel pack that never enters those volumes.

Solution of Equations. A series of nonlinear partial differential equations has been derived that simulates fluid flow and gravel packing in the wellbore model. These equations are composed of state variables that are a function of axial distance and time. A finite-element[19,20] method is used to solve the equations with the Galerkin method of weighted residuals and a piecewise-linear approximation for the axial-distance dependence of state variables. Time derivatives are approximated in the standard difference fashion. Time-dependent quantities are evaluated mostly at the implicit time. The finite-element approximation is solved with the Newton iteration, and the simulation is stepped through discrete intervals of time. The Jacobian matrix is block tridiagonal and is solved with Gaussian elimination.

Gravel-Packing Simulations

Three gravel-packing experiments have been simulated: a circulating pack, a squeeze pack, and a circulating/squeeze pack. Cumulative gravel distributions were matched by simulation. Each match was obtained by adjusting parameters in the simulator that are not known with precision, such as gravel-pack liquid volume fraction and permeability, slurry power-law coefficient, and effective perforation length. Although perforation length is known with precision, the entire perforation may not pack solidly with gravel and a void may be present at the perforation end. The effective perforation length accounts only for the perforation volume that solidly packs with gravel. **Table 1** gives the values of parameters used in the simulations.

Circulating Pack. The first simulation is a circulating pack. Slurry contained 5-lbm/gal gravel, with a liquid solution of 0.06-lbm/gal HEC. The match is shown in **Fig. 4,** and a cross section of the annulus is shown in **Fig. 5**. Gravel-pack liquid volume fraction was 0.39, gravel-pack permeability was 20,000 md, and the slurry power-law coefficient was 12,000 cp-sec^{n-1}. In the interval from 45 to 50 ft in Fig. 5, there is no screen. Gravel is assumed to pack axially, completely filling the annulus. Gravel-pack liquid volume fraction is proportional to the slope of the cumulative gravel distribution in that interval and is within one standard deviation of measurements[21] reported for 40/60-mesh gravel (average liquid volume fraction is 0.398 and standard deviation is 0.028). Slurry viscosity is dependent on gravel concentration, and a sufficiently high gravel concentration can increase slurry viscosity several-fold over the viscosity of liquid alone.[22] The input slurry power-law coefficient is roughly double that for liquid. Gravel-pack permeability is within three standard deviations of reported measurements[21] (average is 69,000 md and standard deviation is 13,600 md). The gravel pack in

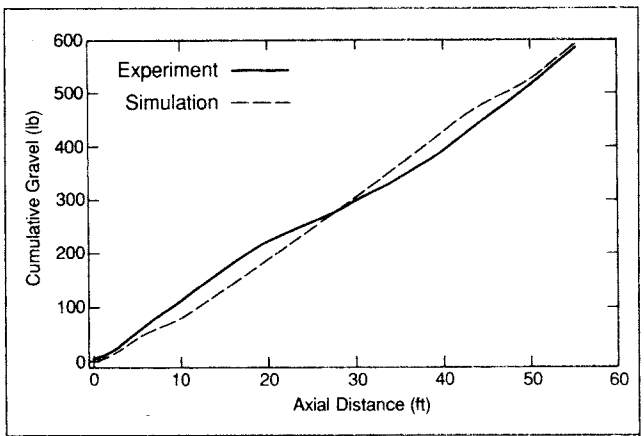

Fig. 8—Match of cumulative gravel distribution for circulating/squeeze configuration.

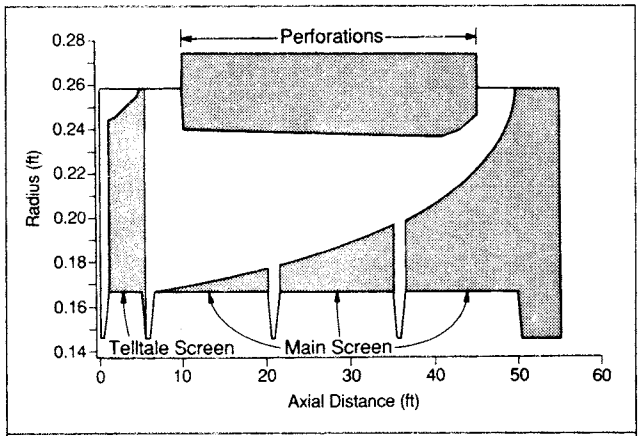

Fig. 9—Cross section of annulus for circulating/squeeze configuration. Shaded area is gravel pack.

the perforation volume (the indented portion from 5 to 40 ft in Fig. 5) does not extend into the annulus. This is consistent with experimental results. Sandout occurred at around 45 ft. Measurements of pressure profile in the wellbore model show a sharp pressure increase at 45 ft that grows with time, demonstrating constriction of a flow channel.

Squeeze Pack. The second simulation is a squeeze pack. Slurry contained 15-lbm/gal gravel, with a liquid solution of 0.08-lbm/gal HEC. The match is shown in **Fig. 6**, and a cross section of the annulus is shown in **Fig. 7**. Gravel-pack liquid volume fraction was 0.44, gravel-pack permeability was 90,000 md, perforation effective length was 0.9 ft, and the slurry power-law coefficient was 56,000 cp-sec^{n-1}. Gravel-pack liquid volume fraction and permeability are within two standard deviations of reported measurements.[21] Input slurry power-law coefficient is roughly four times that of liquid. There is a disagreement between the simulation and the experiment from 0 to 30 ft in Fig. 6. At the time of sandout, observation showed that the bottom 15 ft of the wellbore model contained no gravel. Later, observation showed gravel moving to the bottom of the wellbore model long after the gravel pack was completed. There is also some disagreement from 40 to 45 ft. Experimental and simulated gravel placement differ somewhat. Possible explanations for this are many. Gravel-pack erosion from shear exerted by high-velocity slurry flowing past may be significant, especially when the annulus is almost at sandout. Gravel pack is assumed to be rigid and undeformable, but the pack may be deformed by pressure exerted on it during axial packing, especially if gravel-pack radius decreases sharply away from the interval. Observation confirmed that gravel pack from perforations does not extend into the annulus.

Circulating/Squeeze Pack. The third simulation is a circulating/squeeze pack. Slurry contained 15-lbm/gal gravel, with a liquid solution of 0.08-lbm/gal HEC. The match is shown in **Fig. 8** and a cross section of the annulus is shown in **Fig. 9**. Gravel-pack liquid volume fraction was 0.44, gravel-pack permeability was 20,000 md, perforation effective length was 0.8 ft, and the input slurry power-law coefficient was 49,000 cp-sec^{n-1}, roughly 3.5 times that of liquid. Sandout occurred at two points, first at 5 ft where the telltale screen ends and later at 50 ft where the main screen ends. Very little packing from the telltale screen occurred after the telltale sandout. This was confirmed experimentally. Once sandout occurred at the telltale screen, liquid flow through the washpipe, an indicator of axial packing from the telltale screen, ceased. Gravel-pack profile from the perforation volume is uniform and extends into the annulus. Experimental results are consistent with this. Observation shows that each perforation inlet is surrounded by a disk of gravel pack several inches in diameter. Perforation flow measurements were uniform over the length of the model, indicating an axially uniform distribution of gravel pack in perforations. There is some disagreement in the cumulative gravel distributions. As in the squeeze-pack example, there is disagreement near where sandout occurs. There is also disagreement in the 5-to-10-ft and 20-to-30-ft intervals. The experimental distribution indicates a relative lack of gravel in the 20-to-30-ft interval and a relative surplus of gravel in the 5-to-10-ft interval; the simulated distribution is the reverse. The surplus of gravel in the 5-to-10-ft interval would occur if there were axial packing from the telltale screen after sandout. This has been shown not to occur. In the experiment, gravel pack appeared to slump down the annulus, filling the volume just beyond the telltale screen and leaving less gravel in the 20-to-30-ft interval.

All simulations were run on a Cray/X-MP computer. The circulating-pack simulation grid consisted of ⅛-ft elements. Eighty seconds of real time, subdivided into 240 timesteps, were simulated with 614 seconds of computer time. The squeeze-pack simulation grid consisted of ¼-ft elements. Sixty seconds of real time, subdivided into 120 timesteps, were simulated with 154 seconds of computer time. The circulating/squeeze-pack simulation grid consisted of ⅛-ft elements. One hundred thirty-two seconds of real time, subdivided into 386 timesteps, were simulated with 701 seconds of computer time.

Application to Gravel Packing in the Field. The formulation presented for numerically simulating gravel packing is generally applicable to the field and to the wellbore model. However, because conditions in the field can differ from those in the wellbore model, modifications to the formulation may be necessary.

1. Fluid leaks off through perforations into the reservoir. Reservoirs often are heterogeneous, with porosity and permeability a function of position. Perforations often are damaged, resulting in a "skin" or low-permeability zone in their vicinity.
2. Fluid flow in the wellbore is a complex phenomenon. Although dense gravel grains may not settle significantly in slurry if the liquid viscosity is sufficiently high, injected slurry can be heavier than the wellbore fluid and significant gravity segregation can occur, especially in a long wellbore.
3. A significant temperature difference exists between many reservoirs and the surface. Fluid properties, such as density and viscosity, are temperature-dependent.
4. Fluid flow in the wellbore is influenced by wellbore inclination.

Accurately simulating gravel packing in the field may require that some of the factors mentioned above be taken into account.

Conclusions

1. A finite-element, numerical simulator was developed that simulates initial gravel placement in a wellbore.
2. Cumulative gravel distributions obtained from experiment were matched by the simulator.
3. The simulator accurately predicts the location of voids, point of sandout, and degree of gravel packing in perforations and on the annulus.
4. The simulator predicts initial gravel packing; postpacking gravity effects, such as slumping or gravel leakage from perforations, can be estimated from simple mass balance.
5. The simulator can be used for various wellbore configurations.

Nomenclature

A_{cxn} = cross-sectional area of annulus, ft^2
A_j = coefficient of jth resistor in series, ft^{2n}/psi
g = gravitational constant,, 32.174 ft/sec^2
g_c = Newton's law conversion factor, 32.174 lbm-ft/lbf-sec^2
k = permeability, md
K = power-law coefficient, cp-sec^{n-1}
$\dot{m}$ = rate of mass exchange, lbm/ft-sec
$\dot{m}_p$ = rate of liquid exchange, lbm/ft-sec
n = power-law exponent
p = pressure, psi
q = radial volumetric flow rate, ft^2/sec
q_z = axial volumetric flow rate, ft^3/sec
r = radial coordinate, ft
t = time, seconds
v_r = radial velocity, ft/sec
y = volume fraction
z = axial coordinate, ft
z_f = axial coordinate gravel-pack leading surface, ft
$\dot{\gamma}$ = shear rate, seconds^{-1}
θ = inclination from vertical, rad
μ = viscosity, cp
μ_{max} = low shear rate viscosity for power-law fluid, cp
ρ = density, lbm/ft^3

Subscripts

e = effective
g = gravel
i = inner radius of annulus
L = liquid
o = outer radius of annulus
0 = beginning of simulation

Superscript

p = gravel pack

Authors

Schroeder

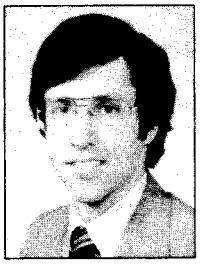

Winterfeld

Phillip H. Winterfeld is a senior engineer at Marathon Oil Co.'s Petroleum Technology Center in Littleton, CO. He holds a BS degree from Massachusetts Inst. of Technology and a PhD degree from the U. of Minnesota, both in chemical engineering. Donald E. Schroeder Jr. has worked for Marathon Oil Co. for 23 years and is currently an advanced senior engineer. He earned BS and MS degrees from the U. of North Dakota, both in chemical engineering. He is project manager for the Horizontal Well Gravel Pack Program initiated through the Completion Engineering Assn. and is currently a member of the SPE Reprint Series Committee.

Acknowledgment

We thank Marathon Oil Co. for permission to publish this paper.

References

1. Spreux, A., Georges, C., and Lessi, J.: "Most Problems in Horizontal Completions are Resolved," *Oil & Gas J.* (June 13, 1988) 48–52.
2. Sparlin, D.D. and Hagen, R.W.: "Controlling Sand in a Horizontal Completion," *World Oil* (Nov. 1988) 54–60.
3. Gruesbeck, C. and Collins, R.E.: "Particle Transport Through Perforations," *SPEJ* (Dec. 1982) 857–65.
4. Gruesbeck, C., Salathiel, W.M., and Echols, E.E.: "Design of Gravel Packs in Deviated Wellbores," *JPT* (Jan. 1979) 109–215.
5. Haynes, C.D. and Gray, K.E.: "Sand Particle Transport in Perforated Casing," *JPT* (Jan. 1974) 80–84.
6. Hodge, R.M.: "Gravel Transport in Deviated Wellbores," paper SPE 10654 presented at the 1982 SPE Formation Damage Symposium, Lafayette, LA, March 24–25.
7. Peden, J.M., Russell, J., and Oyeneyin, M.B.: "Design of an Effective Gravel Pack for Sand Control: A Numerical Approach," paper SPE 13647 presented at the 1985 SPE California Regional Meeting, Bakersfield, March 27–29.
8. Penberthy, W.L.: "Gravel Placement Through Perforations and Perforation Cleaning for Gravel Packing," *JPT* (Feb. 1988) 229–36.
9. Shryock, S.G., Dunlap, R.G., and Milhone, R.S.: "Preliminary Results From Full-Scale Gravel Packing Studies," *JPT* (June 1979) 669–75.
10. Shryock, S.G.: "Gravel-Packing Studies in a Full-Scale, Deviated Model Wellbore," *JPT* (March 1983) 603–09.
11. Skaggs, B.C.: "Transport Efficiency of High-Density Gravel Packing Slurries," paper SPE 12480 presented at the 1984 SPE Formation Damage Control Symposium, Bakersfield, CA, Feb. 13–14.
12. Peden, J.M., Russell, J., and Oyeneyin, M.B.: "A Numerical Approach to the Design of a Gravel Pack for Effective Sand Control in Deviated Wells," paper SPE 13084 presented at the 1984 SPE Annual Technical Conference and Exhibition, Houston, Sept. 16–19.
13. Daneshy, A.A.: "Numerical Solution of Sand Transport in Hydraulic Fracturing," paper SPE 5636 presented at the 1975 SPE Annual Technical Conference and Exhibition, Dallas, Sept. 28–Oct. 1.
14. Wahlmeier, M.A. and Andrews, P.W.: "Mechanics of Gravel Placing and Packing: A Design and Evaluation Approach," *SPEPE* (Feb. 1988) 69–82.
15. Schroeder, D.E. Jr.: "Gravel-Pack Studies in a Full-Scale, High-Pressure Wellbore Model," paper SPE 16890 presented at the 1987 SPE Annual Technical Conference and Exhibition, Dallas, Sept. 27–30.
16. Fredrickson, A.G. and Bird, R.B.: "Non-Newtonian Flow in Annuli," *Ind. & Eng. Chem.* (March 1958) 347–52.
17. Bird, R.B., Stewart, W.E., and Lightfoot, E.N.: *Transport Phenomena*, John Wiley & Sons, New York City (1960) 206.
18. Ikoku, C. and Ramey, H.J. Jr.: "Transient Flow of Non-Newtonian Power-Law Fluids in Porous Media," *SPEJ* (June 1979) 164–74.
19. Zienkiewicz, O.C.: "The Finite Element Method in Engineering Science," McGraw-Hill Book Co., London (1971).
20. Stang, G. and Fix, G.J.: *An Analysis of the Finite Element Method*, Prentice-Hall Inc., Englewood Cliffs, NJ (1973) 116–25.
21. Sparlin, D.D.: "Sand and Gravel—A Study of Mixture Permeabilities," paper SPE 4772 presented at the 1974 SPE Formation Damage Control Symposium, New Orleans, Feb. 7–8.
22. Jennings, A.R. Jr.: "Use of Field Data in the Analysis of the Influence of Proppants on Apparent Fracturing Fluid Viscosity," paper SPE 20641 presented at the 1990 SPE Annual Technical Conference and Exhibition, New Orleans, Sept. 23–26.

SI Metric Conversion Factors

bbl	×	1.589 873	E−01	= m^3
cp	×	1.0*	E−03	= Pa·s
ft	×	3.048*	E−01	= m
ft^3	×	2.831 685	E−02	= m^3
in.	×	2.54*	E+00	= cm
psi	×	6.894 757	E+00	= kPa
lbm	×	4.535 924	E−01	= kg
gal	×	3.785 412	E−03	= m^3
md	×	9.869 233	E−04	= μm^2

*Conversion factor is exact.

SPEPE

Original SPE manuscript received for review Oct. 9, 1989. Revised manuscript received March 2, 1992. Paper accepted for publication Nov. 6, 1991. Paper (SPE 19753) first presented at the 1989 SPE Annual Technical Conference held in San Antonio, Oct. 8–11.